AECL--9952

CA9200221

AECL-9952

ATOMIC ENERGY OF CANADA LIMITED

L'ÉNERGIE ATOMIQUE DU CANADA LIMITÉE

LOCALIZED CORROSION OF ALLOYS C-276 AND 625 IN AERATED SODIUM CHLORIDE SOLUTIONS AT 25 TO 200°C

CORROSION LOCALISÉE DES ALLIAGES C-276 ET 625 DANS LES SOLUTIONS OXYGÉNÉES DE CHLORURE DE SODIUM À UNE TEMPÉRATURE DE 25 À 200°C

J. Postlethwaite

Whiteshell Laboratories
Pinawa, Manitoba R0E 1L0

Laboratoires de Whiteshell

December 1991 décembre

AECL RESEARCH

LOCALIZED CORROSION OF ALLOYS C-276 AND 625 IN AERATED SODIUM CHLORIDE SOLUTIONS AT 25 TO 200°C

by

J. Postlethwaite*

* Corrosion Laboratories
Department of Chemical Engineering
University of Saskatchewan
Saskatoon, Saskatchewan S7N 0W0

Whiteshell Laboratories
Pinawa, Manitoba ROE 1LO
1991

AECL-9952

CORROSION LOCALISÉE DES ALLIAGES C-276 ET 625 DANS LES SOLUTIONS OXYGÉNÉES DE CHLORURE DE SODIUM À UNE TEMPÉRATURE DE 25 À 200°C

par

J. Postlethwaite

RÉSUMÉ

On a identifié antérieurement deux alliages de nickel au molybdène, l'Alliage C-276 et l'Alliage 625, considérés comme métaux candidats pour la fabrication de conteneurs dans le cadre du Programme canadien de gestion des déchets de combustible nucléaire. Du fait de la pauvreté des données sur le comportement sous corrosion localisée de ces alliages passifs dans des conditions qu'on peut rencontrer en enceinte de stockage permanent, on entreprend ce projet pour étudier la corrosion par fissures et piqûres des alliages C-276 et 625 dans les solutions chlorurées à des températures élevées.

On a exécuté des essais électrochimiques et d'immersion dans des solutions neutres de chlorure de sodium (de 0,1% en poids au point de saturation) à une température de 25 à 200°C pour tenter d'identifier les conditions dans lesquelles la corrosion localisée se produit et établir le rapport entre le comportement réel sous corrosion et le comportement prévu d'après les études électrochimiques. Les études de polarisation cyclique montrent que les potentiels de rupture sous passivation passent rapidement à des valeurs plus actives lorsque la température augmente. Au-dessus de 100°C, la résistance à la corrosion localisée diminue considérablement. On présente les résultats des essais d'immersion sous la forme de diagrammes de T en fonction de $[Cl^-]$. Ces diagrammes de susceptibilité (sensibilité) laissent supposer qu'il y a une limite de température de corrosion par fissures pour chaque alliage dans les solutions neutres oxygénées de chlorure de sodium. Au-dessous de cette température, la corrosion ne se produit pas, quelle que soit la concentration de chlorure. Les valeurs de la limite de température de corrosion par fissures s'échelonnent entre 100 et 115°C pour l'Alliage 625. Ces valeurs laissent supposer que la saturation des solutions chlorurées par ébullition superficielle pourrait se produire sans l'amorçage de la corrosion localisée. Ces résultats d'essais électrochimiques indiquent qu'il pourrait y avoir une grande marge de sûreté quant à la susceptibilité à la corrosion localisée au-dessous de 100°C.

EACL Recherche
Laboratoires de Whiteshell
Pinawa, Manitoba R0E 1L0
1991

AECL-9952

LOCALIZED CORROSION OF ALLOYS C-276 AND 625 IN AERATED SODIUM CHLORIDE SOLUTIONS AT 25 TO 200°C

by

J. Postlethwaite

ABSTRACT

Two molybdenum-bearing nickel alloys, Alloy C-276 and Alloy 625, were previously identified for consideration as candidate container materials for the Canadian Nuclear Fuel Waste Management Program. Because of the paucity of data for the localized corrosion behaviour of these passive alloys under conditions that may be experienced in a disposal vault, this project was undertaken to study the crevice and pitting corrosion of Alloys C-276 and 625 in chloride solutions at elevated temperatures.

Electrochemical and immersion tests have been conducted in neutral sodium chloride solutions (0.1 wt% to saturated) at 25 to 200°C, in an attempt to identify the conditions under which localized corrosion occurs and to relate the actual corrosion behaviour to that expected on the basis of electrochemical studies. Cyclic polarization studies showed that the passivation breakdown potentials move rapidly to more active values with increasing temperatures. Above 100°C the resistance to localized corrosion is greatly reduced. The results of the immersion tests are presented in the form of T versus [Cl^-] diagrams. These susceptibility diagrams suggest that there is a limiting crevice-corrosion temperature for each alloy in aerated, neutral sodium chloride solutions. Below this temperature corrosion does not occur, regardless of the chloride concentration. The values of the limiting crevice-corrosion temperatures were in the range 100 to 125°C for Alloy C-276 and 100 to 115°C for Alloy 625. Such values suggest that saturation of the chloride solutions by surface boiling could occur without the initiation of localized corrosion. These electrochemical results indicate that a large safety margin for susceptibility to localized corrosion might be found below 100°C.

AECL Research
Whiteshell Laboratories
Pinawa, Manitoba ROE 1LO
1991

AECL-9952

CONTENTS

		Page
	FOREWORD	i
1.	INTRODUCTION	1
	1.1 BACKGROUND	1
	1.2 SCOPE OF THE INVESTIGATION	1
2.	REVIEW OF THE CORROSION RESISTANCE OF ALLOYS C-276 AND 625	2
	2.1 TEMPERATURE	3
	2.2 AERATION	3
	2.3 OXIDIZING AGENTS	3
	2.4 pH	4
	2.5 STRESS-CORROSION CRACKING	4
	2.6 THERMAL EFFECTS	5
3.	EXPERIMENTAL	5
	3.1 MATERIALS	5
	3.1.1 Test Specimens	5
	3.1.2 Test Solutions	6
	3.2 APPARATUS	6
	3.2.1 Corrosion Test Vessels	6
	3.2.2 Electrochemical Equipment	6
	3.3 PROCEDURES	7
	3.3.1 Cyclic Polarization Tests	7
	3.3.2 Immersion Tests	7
	3.3.3 Specimen Examination	7
4.	RESULTS AND DISCUSSION	7
	4.1 ELECTROCHEMICAL TESTS	7
	4.2 IMMERSION TESTS	9
	4.2.1 Creviced Samples	9
	4.2.2 Corrosion Potential (E_{CORR}) as a Function of Time	9
	4.3 CORROSION MECHANISM	9
5.	NICKEL ALLOYS AND NUCLEAR WASTE CONTAINERS	11
	5.1 LIMITING CREVICE-CORROSION TEMPERATURE	11
	5.2 EFFECTS OF HYDROLYSIS, RADIOLYSIS AND IMPURITIES	11

continued...

CONTENTS (concluded)

		Page
	5.2.1 Hydrolysis	11
	5.2.2 Gamma Irradiation	11
	5.2.3 Impurities	12
	5.3 MATHEMATICAL MODELLING	12
6.	CONCLUSIONS	12
	REFERENCES	13
	TABLES	16
	FIGURES	31

FOREWORD

This work was performed under contract to AECL between 1982 and 1986. The AECL Project Officers were P. McKay and F. King. The work represents part of the Container Materials Evaluation Program of the Canadian Nuclear Fuel Waste Management Program.

1. INTRODUCTION

1.1 BACKGROUND

In 1981, Nuttall and Urbanic [1] included two nickel-based alloys, Hastelloy Alloy C-276 (N10276)[1] and Inconel Alloy 625 (N06625)[2] in a list of alloys recommended for further consideration as possible container materials in the Canadian Nuclear Fuel Waste Management Program (CNFWMP).

The disposal concept involves the burial of the used-fuel waste containers within plutonic rock in the Canadian Shield [2]. One of the factors that could determine whether 500 years of containment [1] can be achieved will be the occurrence of localized corrosion in the form of pitting or crevice corrosion. Passive metals such as Alloy C-276 and Alloy 625 rely on the presence of a thin oxide film for their resistance to corrosion. Halide ions, notably chloride ions, can partially destroy such films, leading to pitting corrosion on freely exposed surfaces or to crevice corrosion in areas of restricted access for dissolved oxygen [3,4].

The groundwater in the Canadian Shield may have a high chloride content [5], and given the paucity of data for the localized corrosion of nickel-based alloys [1,3] in chloride solutions at the temperatures expected at the container surface, it was decided to initiate the present investigation.

An initial contract was awarded to the University of Saskatchewan in 1982, which was renewed in 1983, 1984 and 1985, and this report presents the results of those investigations.

1.2 SCOPE OF THE INVESTIGATION

At the time of the Nuttall and Urbanic [1] report, it was assumed for the purposes of assessment "that the container-skin temperature will be 150°C or less." The maximum container-skin temperature since specified for the Used Fuel Disposal Centre [6] is 100°C.

The "probable" groundwater composition in the crystalline rocks of the Canadian Shield (given by Nuttall and Urbanic) indicated chloride ion concentrations in the range from 20 to 100 mg/L, with a maximum value of 400 mg/L. It is now known that these values may be greatly exceeded [5,7], with chloride ion concentrations in the range from 10^4 to 10^5 mg/L, at a depth of 1000 m (Figure 1). Another factor to be taken into account when considering possible salt concentrations in the groundwater is the possibility of boiling at the container surface prior to the establishment of the full hydrostatic head of water [8].

---

[1] Trademark of Haynes International Inc.
[2] Trademark of Inco Alloys International Inc.

Dissolved oxygen, which plays an important role in the localized corrosion of passive metals, may be present in small amounts in the groundwater, especially in the absence of H_2S [1,9-11]. Oxygen will be introduced as a result of the burial operations [7], and could also be formed as a result of water radiolysis [12].

The limited knowledge of the localized corrosion behaviour of Alloy C-276 and Alloy 625 at the outset of this project is illustrated by the temperature/chloride ion crevice-corrosion diagram for a variety of materials (Figure 2) presented by Nuttall and Urbanic. The paucity and disparate nature of the data are obvious.

In this report we present the results of a series of immersion tests designed to determine more definitive $T/[Cl^-]$ susceptibility diagrams for crevice corrosion of the two alloys in aerated solutions. The tests have been conducted over a wide range of temperatures (25°C to 200°C) and chloride concentrations (0.1 wt% NaCl to saturation). The results of electrochemical tests performed to determine the mechanisms of the corrosion processes are also reported. A literature survey and brief discussion of other forms of corrosion is also included.

2. REVIEW OF THE CORROSION RESISTANCE OF ALLOYS C-276 AND 625

Nickel-based alloys that have both high chromium and molybdenum contents are resistant to corrosion in a wide range of oxidizing and reducing environments [3]. They exhibit good resistance to uniform and localized corrosion in chloride solutions and to stress-corrosion cracking (SCC). This resistance to SCC is attributed to the high nickel content.

Alloy 625 has superior mechanical properties because of the matrix stiffening effect provided by the additions of niobium and molybdenum to the nickel-chromium matrix [3], whereas Alloy C-276 has superior localized corrosion resistance by virtue of its higher molybdenum and tungsten contents [3]. Alloy C-276 was developed from the original Alloy C by reducing the carbon and silicon contents to produce an alloy less susceptible to the precipitation of the M_6C carbide and the intermetallic μ-phase during welding [14]. Alloy C-4 was a further development with reduced iron, manganese and tungsten contents to further reduce the precipitation of the μ-phase. Alloy C-4 is the preferred version for nuclear fuel waste disposal containers in Europe [15].

Notwithstanding their excellent corrosion resistance in chloride solutions and brines, the Ni-Cr-Mo alloys do suffer accelerated uniform corrosion, localized corrosion (crevicing and pitting) and SCC at elevated temperatures. Besides temperature, the other factors involved are aeration and the presence of other oxidizing agents such as Fe^{3+}, H_2O_2, ClO^-; pH; residual or applied stress; previous thermal history; chloride concentration; and the presence of a tight crevice. The hydrolysis of salts such as $MgCl_2$ leading to a lower pH, and water radiolysis with the formation of oxidizing agents such as O_2, H_2O_2 and ClO^-, must also be taken into consideration for the use of these alloys under nuclear waste disposal conditions.

2.1 TEMPERATURE

Although Alloys C-276 and 625 have excellent resistance to uniform corrosion in hot seawater up to 150°C, both materials suffer crevice attack under these conditions [3]. A summary of plant corrosion tests (Table 1) for a wide variety of process brines illustrates the susceptibility of these alloys to localized corrosion at elevated temperatures. Tests with the Salton Sea geothermal brine at 105 and 232°C [4] (Table 2) illustrate the effect of temperature on uniform and localized corrosion and on SCC. At 105°C the general corrosion rate of both alloys in aerated brine was <1 μm/a and neither localized corrosion nor SCC was observed. However, at 232°C in brine containing 100 $\mu g \cdot g^{-1}$ of dissolved oxygen, the general corrosion rates were enhanced and both localized corrosion and SCC were observed. The rate of general corrosion of plain Alloy C-4 specimens in a quinary salt brine (Q-brine containing 26.8 wt% $MgCl_2$) increased from 0.02 to 0.15 μm/a, in the range 90 to 170°C [16] (Table 3).

2.2 AERATION

There is a major effect of solution aeration on the corrosion of Ni-Cr-Mo alloys. This effect is clearly seen in the Salton Sea geothermal brine results [4] at 232°C (Table 2), and in the results obtained by Braithwaite and Molecke [12] (Table 4). It should be noted that both sets of results show that Alloy 625 suffers pitting corrosion in deaerated high-temperature brines under conditions where Alloy C-276 is resistant to this form of localized attack.

2.3 OXIDIZING AGENTS

The standard test method for pitting and crevice corrosion of stainless steels and related alloys in oxidizing chloride environments (ASTM G48-76) involves the use of a 10 wt% solution of $FeCl_3 \cdot 6H_2O$ (pH 1.6). The minimum temperatures for crevice corrosion (CCT) in this solution are given in Table 5. A comparison between the values of CCT and the temperatures required for pitting in an oxidizing NaCl-HCl solution (pH = 2) are given in Table 6 [15]. Clearly, Alloy C-276 is superior to Alloy 625 on the basis of all these tests.

On the basis of electrochemical tests, Schmitt and Köster [17] concluded that Alloy C-4 can be expected to suffer localized corrosion at temperatures $\geq$55 to 60°C in aqueous solutions containing high concentrations of chloride. The incubation times for such processes could be $\geq$200 d. This temperature is similar to the value of CCT in the standard $FeCl_3$ test. Their electrochemical tests were performed in both Q-brine and 1 $mol \cdot L^{-1}$ NaCl + 10^{-3} $mol \cdot L^{-1}$ HCl (pH = 3). They also studied the effect of other oxidizing agents, including H_2O_2 and ClO^-, which could possibly be produced by water radiolysis at the container surface. The strong local attack observed in immersion tests in Q-brine at T = 90°C in the presence of gamma irradiation (Table 3) [16,18] was attributed to the formation of oxidizing substances, which raise the potential of the metal above the passivation breakdown potential.

2.4 pH

Severe pitting and under-spacer attack were observed [19] for Alloy C following a 73-d test in 20 wt% NaCl brine (pH 2.0 to 4.5) at 74°C. These observations are in contrast to the absence of such corrosion in near-neutral brines at similar temperatures (Table 7).

The $MgCl_2$ brines used in the Karlsruhe studies [18,20] have a low pH at elevated temperatures because of hydrolysis. Thus the Q-brine, with a pH ~3.8 at 90°C causes crevice corrosion with both metal-to-metal and metal-to-PTFE crevices of Alloy C-4 (Table 8). Braithwaite and Molecke [12] (Table 4) concluded that hydrolysis of magnesium salts affected the comparative corrosivity of the brines used in their studies.

Plante et al. [21] measured the current density corresponding to the active/passive transition for various alloys over the pH range from 1 to 7 and ranked the crevice-corrosion resistance (increasing) as follows: 306L, 316L, 825, 625, and C-276. The current at the active/passive transition is an important parameter in the model for crevice corrosion developed by Oldfield and Sutton [22]. These authors studied the active/passive transition in solutions that reflected the changes in $[Cl^-]$ and $[H^+]$ due to ionic migration and diffusional mass transfer within a crevice and not just as a function of pH, as in the study of Plante et al.

2.5 STRESS-CORROSION CRACKING

Alloys C-276 and 625 have excellent resistance to SCC in chloride media, with no cracking being observed in boiling 42 wt% $MgCl_2$ after 1000 h [23]. This resistance is attributed to the high nickel content in these alloys. However, under conditions of high T and $[Cl^-]$, both of these alloys suffer transgranular SCC [4,24] (Table 2). This is the typical mode of cracking for non-sensitized austenitic alloys.

The presence of H_2S exacerbates SCC, as shown by the work of Vaughn and Chaung [25] (Figure 3), with the combination of H_2S and Cl^- creating a synergistic effect. The results for various alloys in 25 wt% NaCl containing no H_2S suggest that Alloys C-276 and 625 should not be attacked at 204°C. Saturation of a 25 wt% NaCl solution with H_2S produced SCC of Alloy C-276 at 177°C and Alloy 625 at 204°C. Alloy 625 was not studied at 177°C. It appears, on the basis of this study, that the critical temperature for SCC of Alloys 625 and C-276 is greater than 150°C in H_2S/Cl^- solutions and >200°C in Cl^- solutions in the absence of H_2S.

Slow strain rate experiments at 90°C for Alloy C-4 under potentiostatic control in Q-brine revealed cracking at potentials <50 mV from the free corrosion potential [20]. It was suggested that SCC under disposal vault conditions, where a shift of potential may occur due to the presence of impurities or oxygen, cannot be excluded. Similar experiments with Alloy C-276 in granitic groundwaters [16] (Figure 4) lead to the conclusion that local acidification, such as could be produced during crevice corrosion, could lead to SCC. Further slow strain rate tests [20] with Alloys C-276 and C-4 in granitic groundwaters containing chloride at 170°C, revealed different behaviour for the two alloys, with Alloy C-276 exhibiting better resistance to SCC.

2.6 THERMAL EFFECTS

Streicher [14] made a comprehensive study of the effects of isothermal heating on the crevice, intergranular and SCC behaviour of Alloys C, C-276, and C-4. The results are summarized in Table 9. Carbon in excess of 0.004 wt% resulted in the intergranular SCC of Alloy C-276 in 45 wt% $MgCl_2$. The time required for cracking decreased with increased carbon content (Table 10). The cracking was related to the presence of the M_6C phase, not the intermetallic phase. The M_6C phase also had an effect on the resistance to pitting and crevice corrosion. In the case of pitting and crevice corrosion, a higher concentration of carbon, up to 0.01 wt%, was considered tolerable.

The TTS (time/temperature/sensitization) studies of Plante and Helie [16] with Alloys C-276 and C-4 clearly indicated the superior resistance of C-4 to intergranular corrosion following heat treatment. However, electrochemical studies suggest, on the basis of the magnitude of the current at the active/passive transition, that both alloys had increased susceptibility to crevice corrosion following a thermal treatment (835°C for 15 min followed by controlled cooling down to 700°C in 25 min) (Figure 5). Since the effect of the heat treatment was limited to a thin superficial layer of the samples, it was concluded that welding and filling the container with vitrified waste will not pose a critical problem with respect to intergranular or crevice corrosion of Alloys C-276 and C-4. A similar thermal treatment was not found to significantly affect the stress-corrosion cracking susceptibility of Alloy 625, Alloy C-276 and Alloy C-4 at 80°C, in granitic groundwater solutions [16].

3. EXPERIMENTAL

Our immersion tests were conducted with specimens fitted with artificial crevices, in order to establish T versus [Cl^-] susceptibility diagrams for crevice corrosion. Electrochemical tests were performed using the cyclic polarization technique, to relate the electrochemical behaviour of the alloys to their corrosion behaviour.

3.1 MATERIALS

3.1.1 Test Specimens

Alloys C-276 and 625 test specimens were machined from plate in the as-received mill-annealed condition. The surfaces were wet-ground on silicon carbide papers down to 600 grade. The alloy compositions are shown in Table 11.

Two types of specimen were used:

a) Plain blocks with dimensions 11 mm x 11 mm x 7 mm thick. These blocks were drilled and tapped and used as electrodes with a PTFE compression gasket, and a PTFE-insulated rod made from the same alloy.

b) Blocks with dimensions 25 mm x 13 mm x 7 mm thick. These blocks were fitted with a radially grooved PTFE washer assembly of 16-mm diameter. This assembly was bolted to the alloy under test. A plain PTFE backing washer of 16-mm diameter was used. The assembly is shown in Figure 6. A torque of 6 N·m was applied during final assembly of these artificial crevices. The initial assembly was done under solution. Some of the specimens fitted with artificial crevice assemblies had a drilled and tapped connection and were used as electrodes.

3.1.2 Test Solutions

The solutions were prepared from doubly distilled water and BDH* analytical-reagent-grade NaCl.

3.2 APPARATUS

3.2.1 Corrosion Test Vessels

For temperatures under 100°C, conventional multinecked 1-L glass corrosion cells were used for both the electrochemical and immersion tests. An external saturated calomel electrode with a solution bridge and a Luggin probe was used for electrochemical measurements. Most of the immersion tests between 100°C and 150°C were done in closed tubular glass cells, with a volume of 75 cm^3, immersed in an oil bath. For T > 150°C, similar glass cells were heated in a 1-L Parr[1] stainless steel autoclave containing water. Some immersion tests at T > 100°C, where the corrosion potential was recorded, were done in a Parr 1-L titanium autoclave, with an external saturated calomel reference electrode connected to the autoclave via a stainless steel tube fitted with a PTFE Luggin probe. The solution bridge contained a string, which passed through a valve. The valve could be opened to fill the bridge with solution and ensure electrolyte continuity. When the valve was subsequently closed on the string, no excessive leakage was obtained. The cyclic polarization scans at T > 100°C were done in the titanium autoclave, with an external Ag/AgCl reference electrode maintained at 25°C and system pressure [26].

3.2.2 Electrochemical Equipment

An EG&G PARC, model 350A, electrochemical corrosion system,[2] with IR compensation, was used for the pitting scans. Corrosion potentials were followed during some of the exposure tests with a recorder used in conjunction with an AIS Floyd Bell, Model BA-1 reference electrode buffer amplifier.[3]

---

* Trade Name, Lot Number 98338/1978 (A.C.S. Specification 783)

1 Parr Instruments Ltd., 211 53 St, Moline, Il, 61265, U.S.A.

2 EG&G Princeton Applied Research, PO Box 2565, Princeton, NJ, 08540, U.S.A.

3 AIS, Floyd Bell Associates Inc., Model BA-1, P.O. Box 1237, Columbus, OH, 43212, U.S.A.

3.3 PROCEDURES

3.3.1 Cyclic Polarization Tests

The cyclic polarization tests were performed in nitrogen-deaerated solution. A polarization rate, dE/dt, of 20 mV/min was used. The scans were started from the corrosion potential, E_{CORR}, and reversed when the current achieved a value of 1 mA/cm^2. The scan was terminated at a potential below E_{CORR}.

3.3.2 Immersion Tests

The immersion tests were done in continuously aerated solutions for $T < 100°C$. At $T > 100°C$ the tests were performed in closed cells with an air space above the liquid. The liquid volume in the latter was 25 cm^3 and the air volume 50 cm^3.

3.3.3 Specimen Examination

The specimens were washed with distilled water, dried after the tests, and examined with a stereomicroscope at magnifications up to 160x. When examination of corrosion pits was required, the corrosion products were removed mechanically or by cleaning in an ultrasonic bath. Some specimens were examined by secondary electron microscopy (SEM).

4. RESULTS AND DISCUSSION

4.1 ELECTROCHEMICAL TESTS

The cyclic polarization method [27,28] was used to determine the susceptibility of the alloys to localized corrosion. Both plain and creviced specimens were used in the initial experiments. It was subsequently found unnecessary to use a crevice assembly in the electrochemical tests, since in every case where localized corrosion occurred at the bolted PTFE crevice assembly, it also occurred at the PTFE compression gasket located at the electrode mount. It is perhaps not surprising that Asphahani [29] coined the term "damaging potential" to describe passivation breakdown potentials rather than use the terms pitting potential or crevice potential, since it is difficult to distinguish between the two forms of attack with cyclic polarization tests. Indeed, the round robin [27] tests carried out in conjunction with the standard cyclic polarization test for localized corrosion (ASTM 661) illustrated this fact very well. The standard test makes no attempt to distinguish between pitting and crevice corrosion.

Three conditions were observed (Figure 7) when the electrode surfaces were examined after the tests:

(i) passivation was maintained with no corrosion;

(ii) crevice corrosion occurred at the PTFE compression gasket at the electrode mount;

(iii) crevice corrosion occurred at the PTFE compression gasket plus pitting on the freely exposed surfaces.

On the basis of these results, Alloy C-276 displayed resistance to localized corrosion that was superior to Alloy 625. It should be remembered that the cyclic polarization test is a severe test involving the polarization of the metal to potentials that may not be achieved under natural conditions. The results in Figure 7 should not be interpreted as representing the corrosion behaviour under normal immersion conditions.

At high temperatures, both alloys exhibited unambiguous classical hysteresis loops (Figure 8 a,b) characteristic of passivation breakdown in the sweep to positive potentials and repassivation on the return sweep to negative potentials. Under these conditions, passivation breakdown potentials, E_b, and repassivation potentials (sometimes called the protection potential), E_p, could be readily determined from the polarization curves. The conversion of the potentials to the SHE(T) scale was achieved using the method given by Macdonald [30]. The thermal junction potentials in the neutral NaCl solutions were assumed to be negligible [31].

At lower temperatures, the polarization curves were more complex, and the determination of E_b and E_p more difficult. The curves exhibited the following characteristics:

(i) the absence of a hysteresis loop (Figure 8c) under conditions where localized attack was found on subsequent examination of the specimen;

(ii) the presence of two transpassive zones (Figure 8d). The lower zone may correspond to the anodic oxidation of molybdenum and the upper zone to the dissolution of chromium [32];

(iii) the presence of reversible behaviour in the chromium dissolution zone on the downward sweep with a hysteresis loop occurring below this reversible section (Figure 8e). This reversible behaviour on the downward sweep was still observed when the sweep was interrupted and the potential held at the most noble value for a period of 4 hours (Figure 8f). This suggests that the reversibility is genuine.

Notwithstanding the difficulties in interpreting the polarization curves at the lower temperature, the overall results showed that the resistance to localized corrosion decreased rapidly as the temperature was raised. This is shown by the fall in the passivation breakdown potentials to more active values as the temperature increases (Figure 9).

At the higher temperatures there was no clear systematic variation of the breakdown potential (E_b) with chloride concentration. Also the values of E_b were similar for the two alloys. This last observation is consistent with those of Bogaerts et al. [33] who reported that: "another remarkable phenomenon is the diminishing difference between the E_b values for the various alloys as the temperature increases." These observations were based on experiments comparing the behaviour of AISI 304 stainless steel, Inconel 600, and Incoloy 800 in 0.1 mol/L KCl solutions. Their absolute

values of E_b at elevated temperatures were similar to those observed in the present study, and to those published by Karaminezhaad-Ranjbar et al. [34] for Inconel 600 in 0.1 mol/L NaCl.

4.2 IMMERSION TESTS

4.2.1 Creviced Samples

The corrosion of both alloys took the form of crevice corrosion with no corrosion observed outside the artificial crevice assembly. The corrosion in the crevices (Figure 10) took the form of localized pitting and was usually found under only one or two of the crevices formed by either the slotted PTFE washer or the PTFE backing washer.

The results of the immersion tests with the creviced specimens are presented in the form of T versus [Cl^-] susceptibility diagrams in Figure 11. From these results, we see that the CCT is a function of the chloride concentration. Corrosion was judged to have occurred when obvious metal loss was observed under microscopic examination at a magnification of 160.

Both alloys appear to exhibit a limiting CCT between 100 and 125°C. Below these temperatures, crevice corrosion does not occur, regardless of the chloride concentration. This result is in general agreement with the results of the electrochemical tests (Figure 9), which showed that the passivation breakdown potentials for all the chloride concentrations studied moved rapidly to more active values with an increase in temperature. If passivation breakdown and localized corrosion are going to occur, they would be expected at temperatures >100°C, where the breakdown potentials have much more active values.

4.2.2 Corrosion Potential (E_{CORR}) as a Function of Time

The value of E_{CORR} for Alloy 625 rose to 0.178 V over the first 12 h of exposure to 20 wt% NaCl at 125°C (Figure 12). This value is well above the electrochemically determined value of 0.5 V for E_b. For times greater than 12 h, E_{CORR} falls rapidly to more active values, indicating the initiation of localized attack. Neither Alloy 625 nor Alloy C-276 were attacked after exposures of 290 and 260 d respectively in 20 wt% NaCl at 95°C (Figure 13). The corrosion potential for Alloy C-276 rose to a maximum value of 0.187 V, which was well below the E_b value of ~0.5 V, and no corrosion was observed. For Alloy 625, E_{CORR} rose to a maximum value of 0.262 V, which is above the E_b value of ~0.21 V. However, no sharp drop in E_{CORR}, which would indicate the initiation of localized corrosion, occurred and the specimen was not corroded. The change in E_b with temperature below 125°C is rapid (Figure 9), and given the variations in E_b from specimen to specimen, the absence of attack in the latter case is understandable.

4.3 CORROSION MECHANISM

Szklarska-Smialowska and Mankowski [35] concluded that a reproducible critical potential for crevice corrosion exists and is more negative than the critical potential for pit nucleation. They considered the crevice corrosion of the five stainless steels studied to be a special kind of pitting corrosion. The morphology of the attack (Figure 10) supports a similar

conclusion in our case. If so, it is not surprising that we observe agreement between the electrochemical results and the immersion tests for the concentrated solutions.

The results for the dilute solutions are more difficult to explain. The E_b values in the dilute solutions (for T > 125°C) were similar to those in concentrated solutions, no systematic variation of E_b with chloride concentration being observed. Yet, crevice corrosion was initiated in the dilute solutions only at much higher temperatures than in the concentrated solutions (Figure 11). Clearly, factors other than the value of E_b and the presence of large hysteresis loops during cyclic polarization are involved.

This lack of agreement between electrochemical and immersion test results at the lower chloride concentrations can be explained qualitatively if we apply the differential aeration cell/acidification theory of crevice corrosion, which was mathematically modelled by Oldfield and Sutton [22]. These authors stated that "bulk chloride level is clearly of extreme importance in determining when, if at all, crevice corrosion will occur." On the basis of their theory, crevice corrosion initiates when the differential aeration cell produces acidification and chloride enhancement in the crevice to the point where the critical crevice solution required to disrupt the stable passive film is produced. The Oldfield-Sutton model was successfully applied to a study of the crevice corrosion of stainless steel in seawater by Kain [36], where the major effect of the bulk concentration of Cl^- was illustrated. On the basis of this model, it must be assumed either that the exposure times at the low chloride concentrations were too short for initiation to occur, or the critical crevice solution could not be attained at any exposure time at these lower temperatures.

Oldfield and Sutton did not consider either passivation breakdown, or protection, potentials to be appropriate parameters for inclusion in their crevice-corrosion model [22]. However, their experimental results with Type 316 stainless steel showed a potential/time relationship characteristic of passivation breakdown [37], although the potentials at which breakdown occurred were lower than those normally associated with the passivation breakdown of 316 stainless steel. Further, the initial stages of the attack were said to take the form of micropits, which only later coalesced to give general corrosion.

As discussed elsewhere [28], the writer considers that crevice corrosion of passive metals in chloride solutions is, in fact, a special form of pitting corrosion and that initiation involves the raising of the potential of the metal above a passivation breakdown potential. This potential may be modified by the presence of the crevice.

The role of passivation breakdown potentials, if any, in crevice corrosion requires further clarification. If the passivation breakdown potential is an important parameter, it should be included in the mathematical modelling of crevice corrosion. As pointed out by Accary [38], advances in mathematical modelling should parallel experimental studies relating to container materials for nuclear waste disposal.

5. NICKEL ALLOYS AND NUCLEAR WASTE CONTAINERS

5.1 LIMITING CREVICE-CORROSION TEMPERATURE

Molybdenum-bearing nickel-based alloys, such as Alloy C-276 and Alloy 625, would be promising materials for nuclear waste containers if it is confirmed that the limiting temperature for crevice corrosion in aerated chloride solutions is above 100°C. The significance of this limiting temperature is that possible Cl^- concentration at the canister surface, due to boiling before the full hydrostatic pressure develops, would not cause localized corrosion.

5.2 EFFECTS OF HYDROLYSIS, RADIOLYSIS AND IMPURITIES

Hydrolysis, radiolysis and the presence of impurities could lower the limiting temperature for crevice corrosion.

5.2.1 Hydrolysis

The $MgCl_2$-rich Q-brine used in the studies at the Karlsruhe Nuclear Research Centre had a pH of 3.8 at 90°C [18]. In these brines, Hastelloy C-4 was found to suffer crevice corrosion [20] at both metal/PTFE and metal/metal contacts after periods of 500 to 600 d. Brines encountered in the Canadian Shield have much lower $MgCl_2$ contents, and hydrolysis is not expected to be a problem.

5.2.2 Gamma Irradiation

Pitting corrosion of plain Hastelloy C-4 specimens was observed in Q-brine at 90°C in the presence of gamma irradiation (10^5 rad/h)* over periods of 300 to 600 d [16]. Also, a Hastelloy C-4 specimen with an "engineered crevice" exposed to a deaerated synthetic granitic groundwater (pH = 9.4, $[Cl^-]$ = 35.5 mg/L) incurred significant crevice and pitting attack [20] where a sealant had exfoliated from the specimen surface during gamma irradiation at ~10^5 rad/h for 111 d.

The effect of radiolysis on localized corrosion has been related [17] to the formation of oxidizing agents such as H_2O_2 and ClO^-. These oxidants can raise the potential of the metal above the passivation breakdown value at temperatures where oxygen cannot do so. Clearly, the effects of gamma-irradiation on the limiting CCT require further study.

One possible solution to the radiolysis problem would be the use of a gamma-radiation shield made of a thick-walled low-cost material, such as mild steel [16]. Also, the cast metal matrix proposed for the CNFWMP may be able to serve such a purpose, in addition to its primary mechanical function [7]. However, it is understood that the level of gamma radiation at the container surface for the Canadian disposal concept will be much lower than that experienced where enriched fuel waste is involved.

---

1 rad = 10 mGy

5.2.3 Impurities

Recent electrochemical studies [17] on the effects of impurities such as Fe^{3+}, Cu^{2+}, and S^{2-} suggest that a full knowledge of the composition of the groundwater is very important in the selection of candidate materials and test conditions for further studies for the CNFWMP.

5.3 MATHEMATICAL MODELLING

Clearly, the data presented here must be supplemented by more extensive long-term testing. As pointed out by Accary [38], experimental studies need to be accompanied by further development of the mathematical modelling of the type developed by Oldfield and Sutton [22]. No corrosion model currently exists that would allow us to predict the extent of localized corrosion over the containment durations required in waste disposal. This is particularly true if alloy aging and/or phase separations occurring over long time periods are to be taken into account [38]. Notwithstanding these difficulties, such an approach is required so that medium- to long-term (10 to 50 year) pilot tests can be extrapolated to the desired 500-year-minimum container lifetime.

6. CONCLUSIONS

1. The crevice corrosion of Alloy C-276 and Alloy 625 in aerated chloride solutions is a special case of pitting corrosion occurring above a passivation breakdown potential, which is modified by the presence of the crevice.

2. Both alloys appear to exhibit a limiting CCT in highly concentrated aerated NaCl solutions. This temperature is in the range from 100 to 125°C for Alloy C-276 and from 100 to 115°C for Alloy 625. These ranges are preliminary and further study is required to establish more exact values.

3. The rapid rise of the passivation breakdown potentials to more noble values below 100°C suggests that a large margin of safety with respect to crevice corrosion exists at such temperatures.

4. The limiting CCT varies with the nature of the oxidizing agent involved, as evidenced by the values of ~45°C and ~60°C obtained for Alloy 625 and Alloy C-276 respectively in 10 wt% $FeCl_3$.

5. Further long-term testing of these alloys should be accompanied by parallel developments of a mathematical model for crevice corrosion, which includes passivation breakdown potentials as a major parameter.

REFERENCES

1. K. Nuttall and V.F. Urbanic, "An Assessment of Materials for Nuclear Fuel Immobilization Containers," Atomic Energy of Canada Limited Report, AECL-6440 (1981).

2. K.W. Dormuth and K. Nuttall, "The Canadian Nuclear Fuel Waste Management Program," Radioactive Waste Management and the Nuclear Fuel Cycle 8, 93 (1987).

3. W.Z. Friend, "Corrosion of Nickel and Nickel Base Alloys," John Wiley and Sons, Inc., New York, 1980.

4. P.F. Ellis II and M.F. Conover, "Materials Selection Guidelines for Geothermal Energy Utilization Systems," U.S. Department of Energy, DOE/RA/27026-1 (1981).

5. P. Fritz and S.K. Frape, "Saline Groundwaters in the Canadian Shield - A First Overview," Chemical Geology 36, 179 (1982).

6. P. Baumgartner and G.R. Simmons, "Disposal Centre Engineering for the Canadian Nuclear Fuel Waste Management Program," Radioactive Waste Management and the Nuclear Fuel Cycle 8, 219 (1987).

7. P.M. Mathew and P.A. Krueger, "Corrosion of Metal Matrices in Oxygenated Canadian Shield Granitic Groundwaters," Atomic Energy of Canada Limited Technical Record, TR-396* (1986).

8. A.A. Bauer, Contribution to discussion in "The Corrosion Performance of Nuclear Fuel Waste Containers," Atomic Energy of Canada Limited Technical Record, TR-340* (1983).

9. Ref. 4, p. 102.

10. B.C. Syrett, D.D. Macdonald and H. Shih, "Pitting Resistance of Engineering Materials in Geothermal Brines - Low Salinity Brines," Corrosion 36, 130 (1980).

11. J. Postlethwaite, L.W. Vigrass, V. Gummadi, R. Neufeld and B.D. Kybett, "Water Chemistry Testing on Western Canadian Geothermal Waters," Energy Research Unit, University of Regina Contribution No. 20 (1980).

12. J.W. Braithwaite and M.A. Molecke, "Nuclear Waste Canister Studies Pertinent to Geological Isolation," Nuclear and Chemical Waste Management 1, 37 (1980).

13. A.I. Asphahani, "Corrosion Resistance of High Performance Alloys," Materials Performance 19, 33 (1980).

14. M.A. Streicher, "Effect of Composition and Structure on Crevice, Intergranular and Stress Corrosion Cracking of Some Wrought Ni-Cr-Mo Alloys," Corrosion 32, 79 (1976).

15. High Performance Materials, Publication No. N 5041 85-06, Vereinigte Deutsche Metallwerke AG, Duisberg, Fed. Rep. Germany (1985).

16. CEC, "Corrosion Behaviour of Container Materials for Geologic Disposal of High Level Waste," Joint Annual Progress Report 1983; Commission of European Communities, Nuclear Science and Technology Report, EUR-9570-EN (1985).

17. R.E. Schmitt and R. Köster, "Electrochemical Corrosion Studies on Metallic Packaging Materials for High-Level Radioactive Waste," Kernforschungszentrum Karlsruhe GmbH, Karlsruhe Report, KfK-4039 (1986).

18. E. Smailos, R. Köster and W. Schwarzkopf, "Corrosion Studies on Packaging Materials for High Level Wastes," EUR 8657 EN, European Applied Research Report - Nuclear Science Technology 5(2), 175 (1983).

19. P.J. Gegner and W.L. Wilson, "Corrosion Resistance of Titanium and Zirconium in Chemical Plant Exposures," Corrosion 15, 341 (1959).

20. B. Haijtink (ed.), "Corrosion Behaviour of Container Materials for Geological Disposal of High Level Waste," Annual Progress Report, 1984, Commission of European Communities, Nuclear Science and Technology, Report EUR-10398-EN (1986).

21. G. Plante, M. Helie, O. Sanatine and A. Cheniere, "Etudes de Corrosion des Matériaux de Conteneurs pour le Stockage des Déchets Radioactifs en Sites Granitiques," Commission des Communautés Européennes, Sciences et Techniques Nucléaires, EUR-8762-FR (1984).

22. J.W. Oldfield and W.H. Sutton, "Crevice Corrosion of Stainless Steels - A Mathematical Model," British Corrosion Journal 13, 13, 1978; "Crevice Corrosion of Stainless Steels - Experimental Studies," British Corrosion Journal 13, 104 (1978).

23. "Hastelloy Alloy C-276," Publication H-2002A, Cabot Wrought Products Division, Cabot Corporation, IN (1983).

24. S.D. Cramer and J.P. Carter, "Corrosion in Geothermal Brines of the Salton Sea Known Geothermal Resource Area," Geothermal Scaling and Corrosion, Eds. Casper and Pinchback, ASTM STP 717, American Society for Testing and Materials, 1980.

25. G.A. Vaughn and H.E. Chaung, "Wireline Materials for Sour Service," Materials Performance 21, 44 (1982).

26. J. Postlethwaite, "Breakdown of Passivity of Nickel in Alkaline-Chloride Solutions at 25-275°C," Electrochimica Acta 12, 333 (1967).

27. R. Baboian and G.S. Haynes, "Cyclic Polarization Measurements - Experimental Procedure and Evaluation of Test Data," ASTM STP 727, American Society for Testing and Materials, 1981.

28. J. Postlethwaite, "Electrochemical Tests for Pitting and Crevice Corrosion Susceptibility," Canadian Metallurgical Quarterly 22, 133 (1983).

29. A.I. Asphahani, "Localized Corrosion of High Performance Alloys," Materials Performance 19, 9 (1980).

30. D.D. Macdonald, "Reference Electrodes for High Temperature Aqueous Systems - A Review and Assessment," Corrosion 34, 75 (1978).

31. D.D. Macdonald, "The Electrochemistry of Metals in Aqueous Solutions at Elevated Temperatures," In Modern Aspects of Electrochemistry, No. 11, Plenum Press, New York, 1975.

32. M.A. Cavanaugh, J.A. Kargol, J. Nickerson and N.F. Fiore, "The Anodic Dissolution of a Ni-Base Superalloy," Corrosion 39, 144 (1983).

33. W.F. Bogaerts, A.A. Van Haute and M.J. Brabers, "Relative Critical Potentials for Pitting Corrosion of 304 Stainless Steel, Incoloy 800 and Inconel 600 in Alkaline High-Temperature Aqueous Solutions," Journal of Nuclear Materials 115, 339 (1983).

34. M. Karaminezhaad-Ranjbar, J. Mankowski and D.D. Macdonald, "Pitting Corrosion of Inconel 600 in High Temperature Chloride Solution under Controlled Hydrodynamic Conditions," Corrosion 41, 197 (1985).

35. Z. Szklarska-Smialowska and J. Mankowski, "Crevice Corrosion of Stainless Steels in Sodium Chloride Solution," Corrosion Science. 18, 953 (1978).

36. R.M. Kain, "Crevice Corrosion Behaviour of Stainless Steels in Sea Water and Related Environments," Corrosion 40, 313 (1984).

37. J. Postlethwaite, B. Huber and D. Makepeace, "Hydrodynamic Effects During Electrochemical and Exposure Pitting Tests with Passive Films," Corrosion 42, 646 (1986).

38. A. Accary, "Corrosion Behaviour of Container Materials for Geological Disposal of High Level Radioactive Waste," Commission of European Communities Report, EUR-9836 (1985).

---

* Unrestricted, unpublished report available from SDDO, AECL Research, Chalk River, Ontario K0J 1J0.

TABLE 1

PLANT CORROSION TESTS OF Ni-Cr-Mo ALLOYS IN AQUEOUS SOLUTION OF NONOXIDIZING CHLORIDE SALTS [3]

Salt Solution (% by wt) and Exposure Conditions	T (°C)	Time (d)	Corrosion Rate (mils/year*)	
			Hastelloy C	Inconel 625
Satd. NaCl brine	71	163	0.02	-
Satd. NaCl brine; Velocity 5.2 ft**/s	88	63	0.1	0.1
Satd. NaCl brine; Velocity 5.3 ft/s	107	63	0.1	0.1
Satd. NaCl brine in circulating piping of a vacuum evaporator	110-121	494	0.1	0.1[a]
Satd. NaCl/KCl brine plus a small amount of $MgCl_2$ and H_2S in discharge from an evaporator	92	42	1.7[b]	3.2[c]
Satd. NaCl brine plus 1.6 to 16 g/L $CaCl_2$; 15 to 100 g/L $CaSO_4$; 0.2 to 20 g/L $MgCl_2$; pH 7.5; Velocity 7 ft/s	124	54	0.1[e]	0.2[f]
51% $MgCl_2$; 1% NaCl; 1% KCl; 2% LiCl; Concentrated from 33% total solubles in an evaporator				
Liquid	166	5	1.0	2.0
Vapour	166	5	0.8	3.0
62% $CaCl_2$ brine	154	56	0.4	-
73% $CaCl_2$ brine	177	36	0.3[g]	-
58 to 71% $CaCl_2$ in an evaporating pan	160-171	60	2.7[h]	-
26 to 31% NH_4Cl; 3/4 immersed in flux tank	88	98	0.4[j]	1.7[k]
30 to 43% NH_4Cl in an evaporator	110	18	6.0	-
Up to 71% $ZnCl_2$ in an evaporator under 28 in. vacuum	107	35	0.1	0.3

* 1 mil/year ≡ 25 μm/a.
** 1 ft = 0.3048 m.
a Perforated by crevice attack under spacer.
b Crevice attack under spacer, 14 mils maximum penetration.
c Pitting in surface, 13 mils max.; Perforated in crevice.
d Pitting in surface, 17 mils max.; Perforated in crevice.
e Pitting, 8 mils in crevice.
f Pitting, 20 mils in crevice.
g Pitting near spacer and at machined edges of specimen.
h Incipient pitting under spacer.
i Perforated at machined edges of specimen.
j Pitting in surface, 12 mils max.
k Perforated by pitting.

TABLE 2

CORROSION RATES MEASURED IN 15-d AUTOCLAVE TESTS IN SYNTHETIC SALTON-SEA GEOTHERMAL BRINE* AT 105°C AND 232°C [4]

(a) 105°C

Material Tested	Deaerated Fluid				Aerated Fluid			
	Uniform Corrosion[a] (mils/year[+])	Pitting[b] (mils/year)	Crevice Corrosion	SCC[c]	Uniform Corrosion[a] (mils/year)	Pitting[b] (mils/year)	Crevice Corrosion	SCC[c]
Inconel 625	<0.05	N	N	N	<0.05	N	N	N
Hastelloy C-276	<0.05	N	N	N	<0.05	N	N	N

(b) 232°C: pressure = 422.6 psia

Material Tested	Deaerated Fluid				Solution Containing 100 μg/g			
	Uniform Corrosion[a] (mils/year)	Pitting[b] (mils/year)	Crevice Corrosion	SCC[c]	Uniform Corrosion[a] (mils/year)	Pitting[b] (mils/year)	Crevice Corrosion (mils/year)	SCC[c]
Inconel 625	<0.05	N	X[e]	X	19.2	530	>5	X
Hastelloy C-276	<0.05	N	N	N	5.9	640	>5	X

Key to Table

N = indicated form of corrosion not detected

X = indicated form of corrosion detected

[+] 1 mil/year ≡ 25 μm/a
[a] Based on weight loss
[b] Based on maximum pit depth
[c] U-bend specimens
[d] Specimens with fabricated crevices
[e] >1 mil/year but <5 mil/year

*

Brine Constituent	mg/L (As prepared)	Brine Constituent	mg/L (As prepared)
Na	59 250	SiO_2	21
Ca	22 400	B	200
K	16 700	Ba	294
Fe	3.9	Li	182
Mn	1 710	Pb	14
Zn	345	Rb	74
Sr	706	Mg	27
Cl	140 200	S	34

TABLE 3

GENERAL AND LOCAL CORROSION ON PLAIN SPECIMENS+ OF HASTELLOY C-4 IN Q-BRINE* [16]

T (°C)	Gamma Irradiation (rad/h)	Test Time (d)	General Corrosion Average Corrosion Rate (μm/a)	Pitting Corrosion Maximum Penetration Rate (μm/a)
90	none	280	0.02 ± 0.02	-
90	none	559	0.02 ± 0.02	-
170	none	212	0.15 ± 0.05	-
170	none	368	0.15 ± 0.05	-
90	10^5	321	3.9 ± 0.11	1100
90	10^5	606	2.3 ± 0.07	450

+ Tested in as-delivered condition.
* Q-Brine: 26.8 wt% $MgCl_2$, 4.7 wt% KCl, 1.4 wt% NaCl, 65.7 wt% H_2O.
- No corrosion attack.

TABLE 4

CORROSION RATES OF ALLOYS 625 and C-276 IN DEOXYGENATED AND OXYGENATED SOLUTIONS AT 250°C [12]

Alloy	Pressure (MPa)	Test Time (d)	Oxygenation	Brine A (mm/a)	Brine B (mm/a)	Seawater (mm/a)
Inconel 625	5	28	Deoxygenated	0.005	0.001	0.012*
Hastelloy C-276	5	28	Deoxygenated	0.007		0.0015
Hastelloy C-276	7	14	600 μg/g	0.06**		
Hastelloy C-276	7	14	1750 μg/g			0.2**

* Pitting Corrosion
** Pitting and Crevice Corrosion

Brine A is a high Mg, K and Na chloride brine ($[Cl^-]$ = 190 000 μg/g; pH 6.5).
Brine B is a near-saturated, predominantly NaCl brine ($[Na^+]$ = 115 000 μg/g; $[Cl^-]$ = 175 000 μg/g; pH 6.5).

TABLE 5

CREVICE-CORROSION TEMPERATURES (°C) IN 10 wt% $FeCl_3$ [1]

Reference	Inconel 625	Hastelloy C-276
Streicher[1]	RT-50*	65-75*
Steigerwald[2]	RT-50*	>50
Tapping[3]	45	

[1] M.A. Streicher, "Development of Pitting Resistant Fe-Cr-Mo Alloys", Corrosion 30, 77 (1974).

[2] F.R. Steigerwald, "New Molybdenum Stainless Steels and Alloys for Corrosion Resistance", Paper presented at NACE, Corrosion/74, Chicago, Ill., 1974, paper No. 44.

[3] R.L. Tapping, Chalk River Nuclear Laboratories, unpublished work (1981).

* T_1-T_2 = resistant at T_1 but not at T_2.

RT Room temperature.

TABLE 6

PITTING AND CREVICE-CORROSION TEMPERATURES IN OXIDIZING NaCl-HCl SOLUTION* [23]

	Pitting Temperature (°C)	Crevice-Corrosion Temperature (°C)
Hastelloy C-276	150	80
Cabot Alloy 625	101	25

* 4 wt% NaCl + 0.1 wt% $Fe_2(SO_4)_3$ + 0.01 mol/L HCl; pH = 2.

TABLE 7

CORROSION OF ALLOY C IN SALT SOLUTIONS [19]

Environment	T/°C	Duration of Test (d)	Corrosion kate (mils/a)*
Sat'd NaCl brine	60	169	0.002[a]
Sat'd KCl brine	60	183	0.002
Sat'd NaCl brine	71	163	0.02
Sat'd NaCl brine; pH 2.0-4.5	74	73	12 0.1[b]

* 1 mil/a ≡ 25 μm/a.
[a] Slight attack under spacer.
[b] One of two specimens suffered severe pitting and under-spacer attack.

TABLE 8

CREVICE CORROSION OF ALLOY C-4 IN Q-BRINE* [20]

Specimen Type	Surface Condition	T (°C)	Time (d)	Max Crevice-Corrosion Depth (μm)
A[1]	as-received[3]	90	582	250[4]
B[2]	as-received[3]	90	489	70[5]
B[2]	as-received[3]	170	286	no attack
B[2]	polished (9-μm diamond paste)	90	266	20[5]
B[2]	polished (9-μm diamond paste)	170	266	no attack

* Q-Brine: 26.8 wt% $MgCl_2$, 4.7 wt% KCl, 1.4 wt% NaCl, 65.7 wt% H_2O.
[1] Simulated crevice by contacting metal/PTFE.
[2] Simulated crevices by contacting metal/metal and tightening with two PTFE nuts and bolts.
[3] Surface etched in H_2SO_4.
[4] At the metal/PTFE interface.
[5] At the metal/metal interface.

TABLE 9

EFFECT OF HEAT TREATMENT ON CORROSION BEHAVIOUR OF ALLOYS C, C-276 AND C-4 [14]

Alloy	Analysis		Heat Treatment[1]	Intergranular Corrosion Test Ratios[2]		Crevice Corrosion in 10 wt% Ferric Chloride[3]	Stress-Corrosion Cracking[4] in 45 wt% $MgCl_2$
	C	Si		Ferric Sulphate (24 h)	"Pure" Sulphuric Acid (8 h)	50°C	155°C
Alloy C	0.05	0.70	Solution annealed	1.0	1.0	None	None
			1 h at 704°C	6.1	12.0	Yes	Yes
			1 h at 870°C	13.3	4.6	Yes	Yes
			1 h at 1038°C	5.4	4.8	Yes	Yes
			Furnace cooled	2.6	2.2	Yes	Yes
			Agglomerating	2.0	7.4	Yes	Yes
Alloy C-276	0.01	0.01	Solution annealed	1.0	1.0	None	None
			1 h at 704°C	1.5	1.2	None	None
			1 h at 870°C	13.8	3.1	None	Yes
			1 h at 1038°C	7.3	1.5	None	None
Alloy C-276	0.008	0.004	Solution annealed	1.0	1.0	None	None
			1 h at 704°C	1.0	1.1	None	Yes
			1 h at 870°C	11.4	1.9	None	Yes
			1 h at 1038°C	10.6	1.3	None	Yes
Alloy C-276	0.004	0.01	Solution annealed	1.0	1.0	None	None
			1 h at 704°C	1.1	1.0	None	None
			1 h at 870°C	14.2	1.9	None	None
			1 h at 1038°C	3.5	1.2	None	None
			Furnace cooled	2.4	1.0	None	None
			Agglomerating	2.0	1.0	None	None
Alloy C-4	0.006[5]	0.04	Solution annealed	1.0	1.0	Yes	None
			1 h at 870°C	2.4-7.4	1.3	Yes	None
			Furnace cooled	1.0	1.0	Yes	None

[1] Heat treatments: Furnace-cooled from 1204°C or 1224°C to 538°C in 90 min. Agglomerating - American Oil Company. Thermal cycle: heat in 4 h to 1171°C; hold 1 h; cool to 1121°C and hold 3 h; then cool to 566°C in less than 30 min.

[2] Ratio of corrosion rate of given specimen divided by corrosion rate of solution annealed specimen in boiling 50 wt% H_2SO_4, with and without ferric sulphate.

[3] Specimen with six crevices.

[4] U-bend specimens.

[5] Alloy contains 0.43 wt% Ti to stabilize carbon.

TABLE 10

STRESS-CORROSION CRACKING OF C-276 ALLOYS IN $MgCl_2$ TEST [14]

Alloy	Carbon Content wt%	Heat Treatment	Boiling 45 wt% $MgCl_2$ Test[1]		
			Cracking	Time (hours)	Type of Cracking
Alloy C-276	0.004	As-received	No	2407	
		1 h at 704°C. WQ	No	2407	
		1 h at 870°C. WQ	No	2407	
		1 h at 1038°C. WQ	No	2407	
		1 h at 1224°C. WQ	No	2407	
		Furnace-cooled	No	2407	
		Agglomerating[2]	No	2407	
Alloy C-276	0.005	1 h at 870°C. WQ	No	2407[3]	
Alloy C-276	0.006	1 h at 870°C. WQ	Yes	2414	
Alloy C-276	0.008	1 h at 704°C. WQ	Yes	2252	
		1 h at 870°C. WQ	Yes	957	Intergranular
		1 h at 1038°C. WQ	Yes	4359	Intergranular
		1 h at 1149°C. WQ	No	2847	
Alloy C-276	0.01	1 h at 704°C. WQ	No	6536	
		1 h at 870°C. WQ	Yes	905-2100	
		1 h at 1038°C. WQ	No	6536	

[1] U-bend specimens.
[2] See Table 9 footnotes.
[3] A small crack appeared in this specimen after 3371 h.
WQ ≡ water-quenched.

TABLE 11

NICKEL ALLOY ANALYSES

Alloy	Composition (wt%)															
	Ni	Cr	Mo	Fe	C	Mn	Si	S	Nb + Ta	P	V	W	Co	Al	Ti	UNS No
C-276	Bal	15.70	15.69	6.06	0.002	0.47	0.02	0.002	-	0.008	0.14	3.65	1.87	-	-	N10276
625	60.80	21.63	8.52	4.68	0.03	0.10	0.31	0.001	3.54	0.009	-	-	-	0.14	0.24	N06625

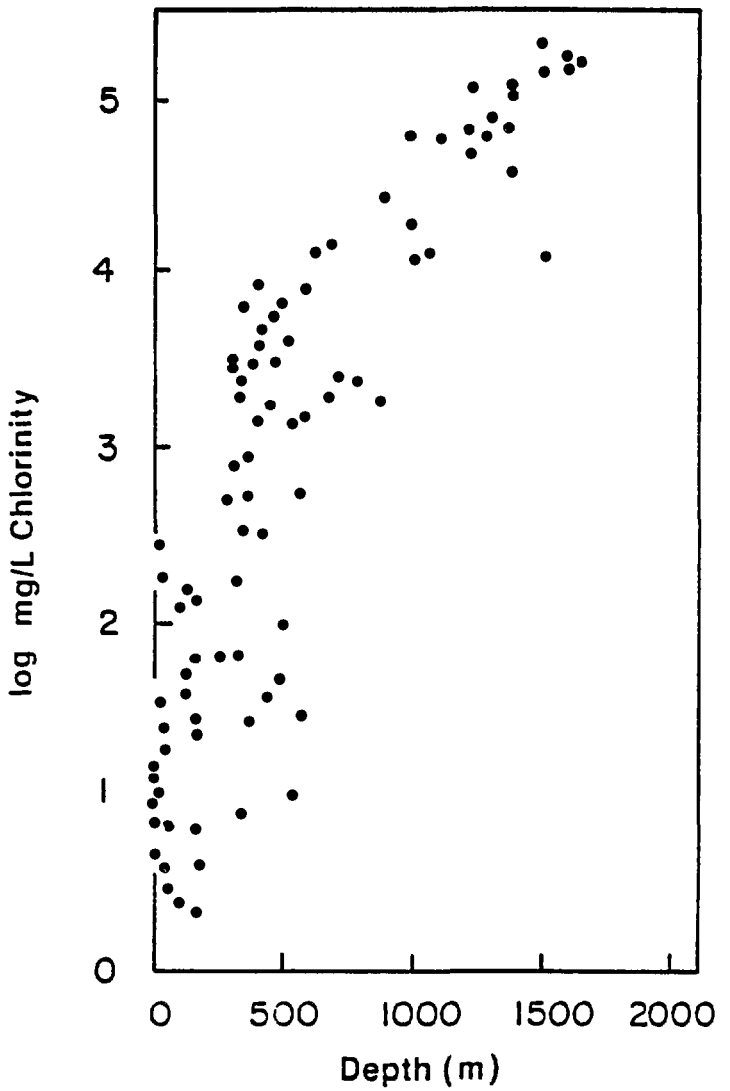

FIGURE 1: Chlorinity of Canadian Shield Groundwaters as a Function of Depth [7]

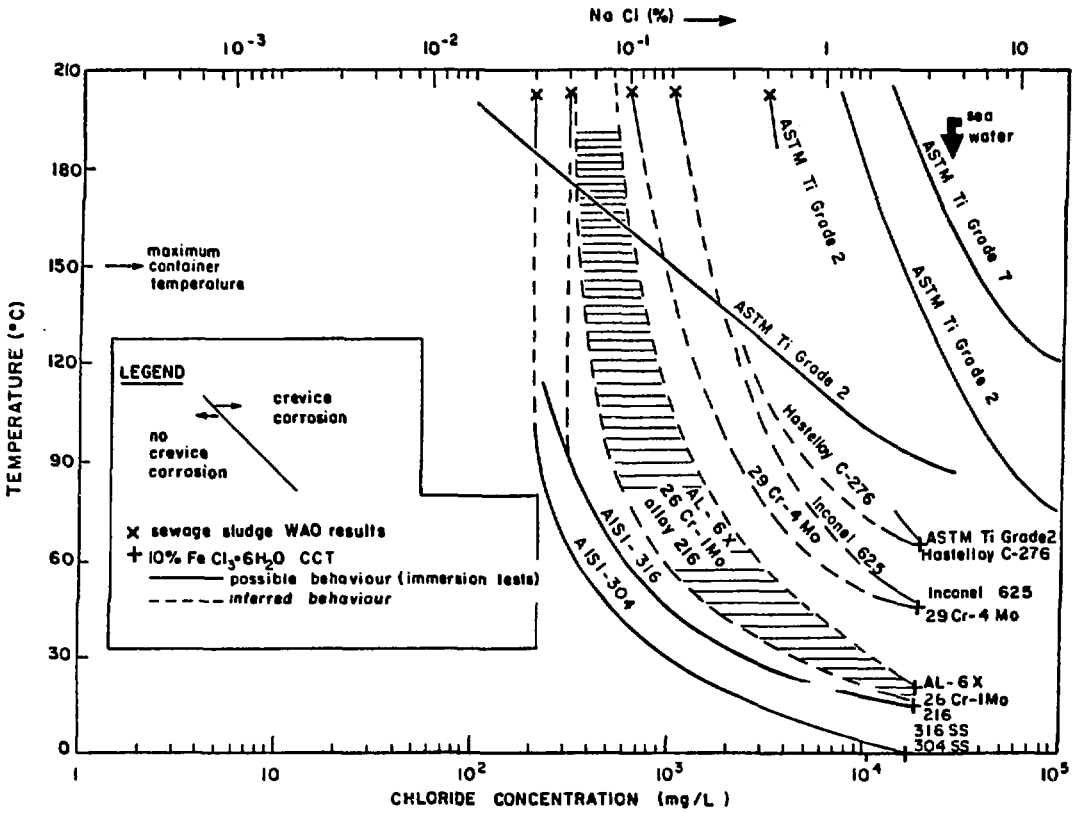

FIGURE 2: Susceptibility Diagrams for the Crevice Corrosion of Various Alloys in Aqueous Chloride Solutions [1]

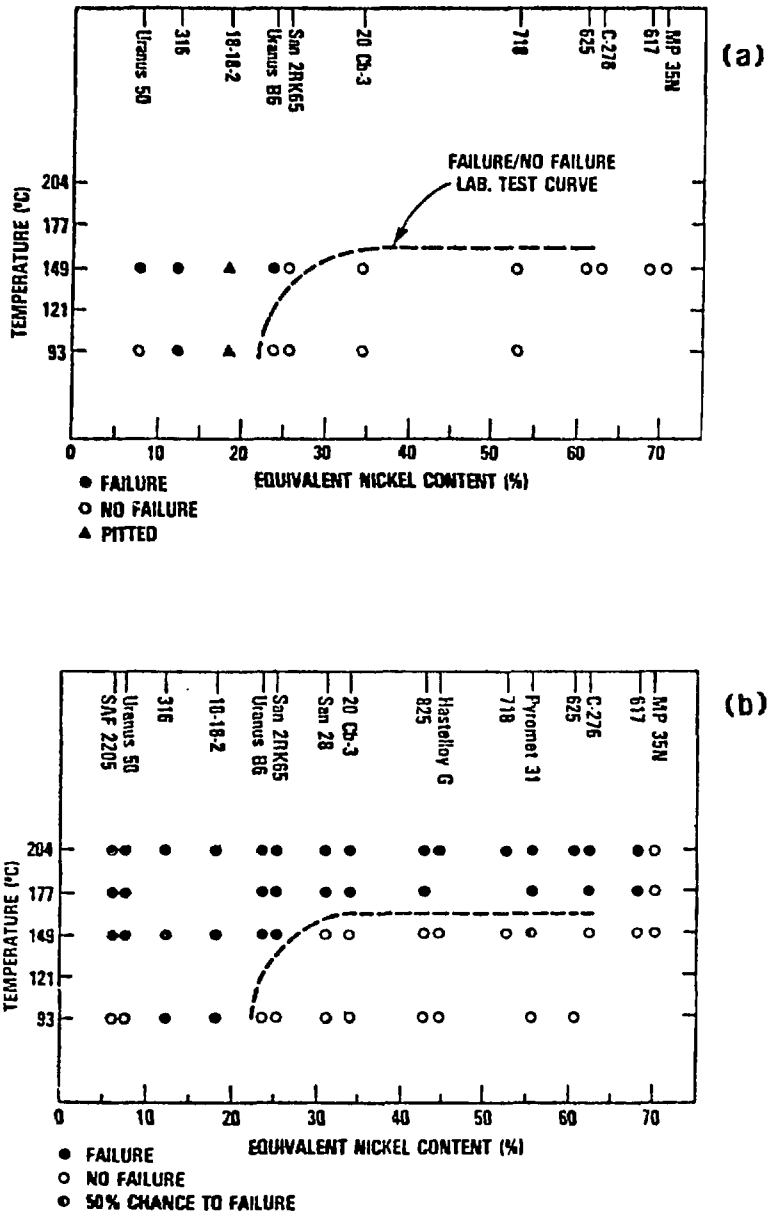

FIGURE 3: Effect of Equivalent Nickel Content (Ni + Co) on SCC Resistance of Wireline Materials [25].

(a) Laboratory environment: 25 wt% NaCl (180 000 mg/L Cl^-), 0.5 wt% acetic acid, saturated with H_2S, pH 3 to 3.5.

(b) Field environment: NaCl, $MgCl_2$, $CaCl_2$,(206 000 mg/L Cl^-), pH 5.7, saturated with field gas (11% H_2S, 40% CO_2, balance C_1-C_{10} hydrocarbons).

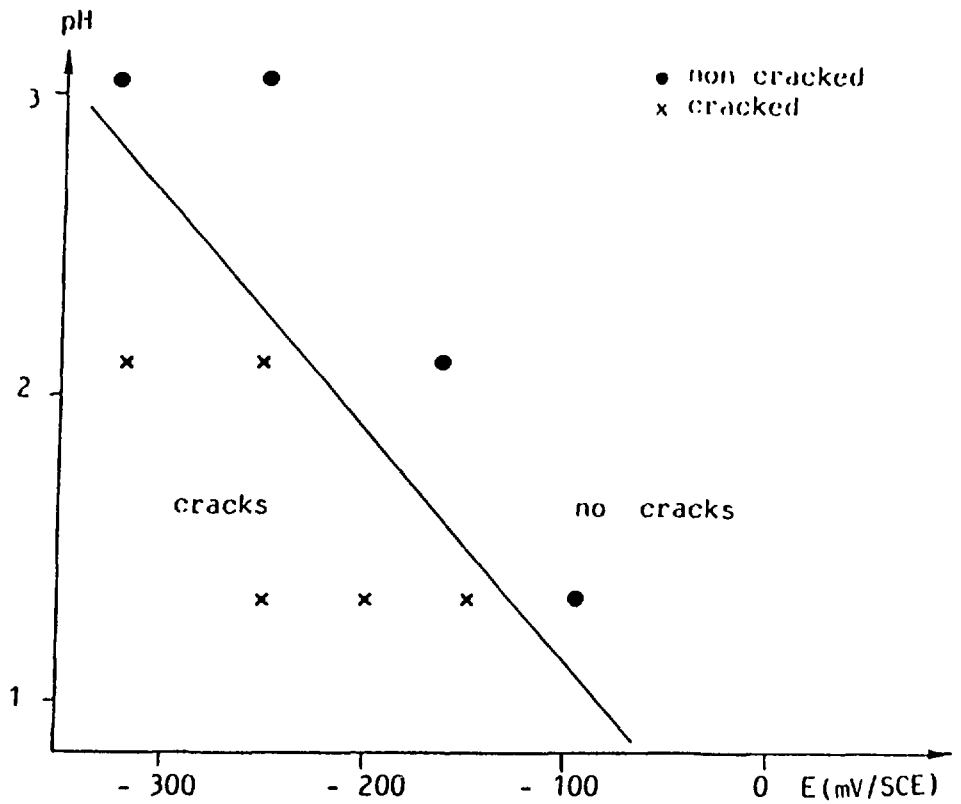

FIGURE 4: Stress-Corrosion Cracking Susceptibility of Alloy C-276 in Granitic Solution, under Controlled Potential, Slow Strain Rate Conditions; Strain Rate = 10^{-6} s^{-1}; $[Cl^-]$ = 0.05 mol/L; T = 80°C [16]

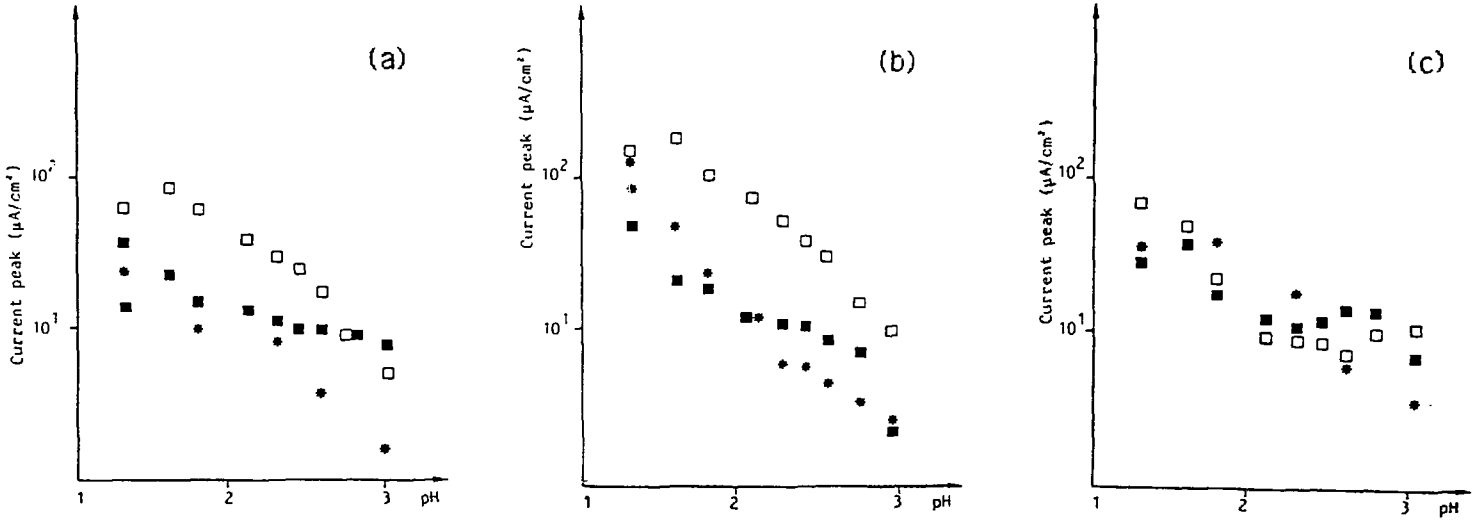

FIGURE 5: Influence of Thermal Treatment on the Crevice Corrosion Susceptibility in Granitic Solution ($[Cl^-]$ = 0.5 mol/L) [16]; (a) Alloy C-276; (b) Alloy C-4; (c) Alloy 625

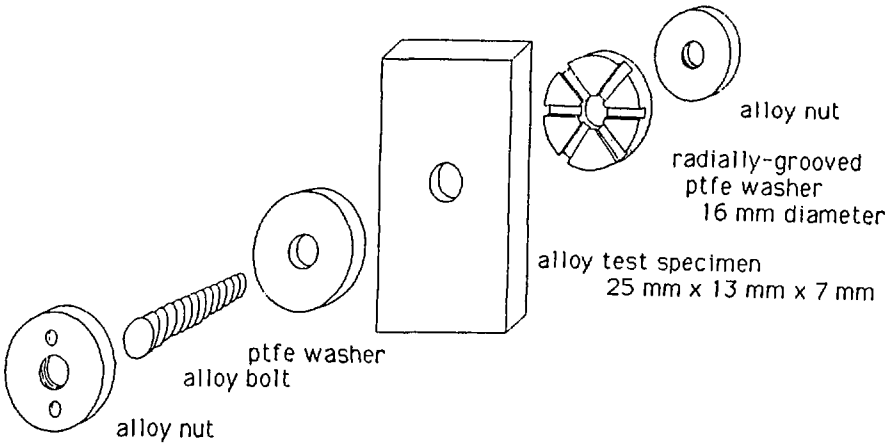

FIGURE 6: Test Specimen with Crevice Assembly

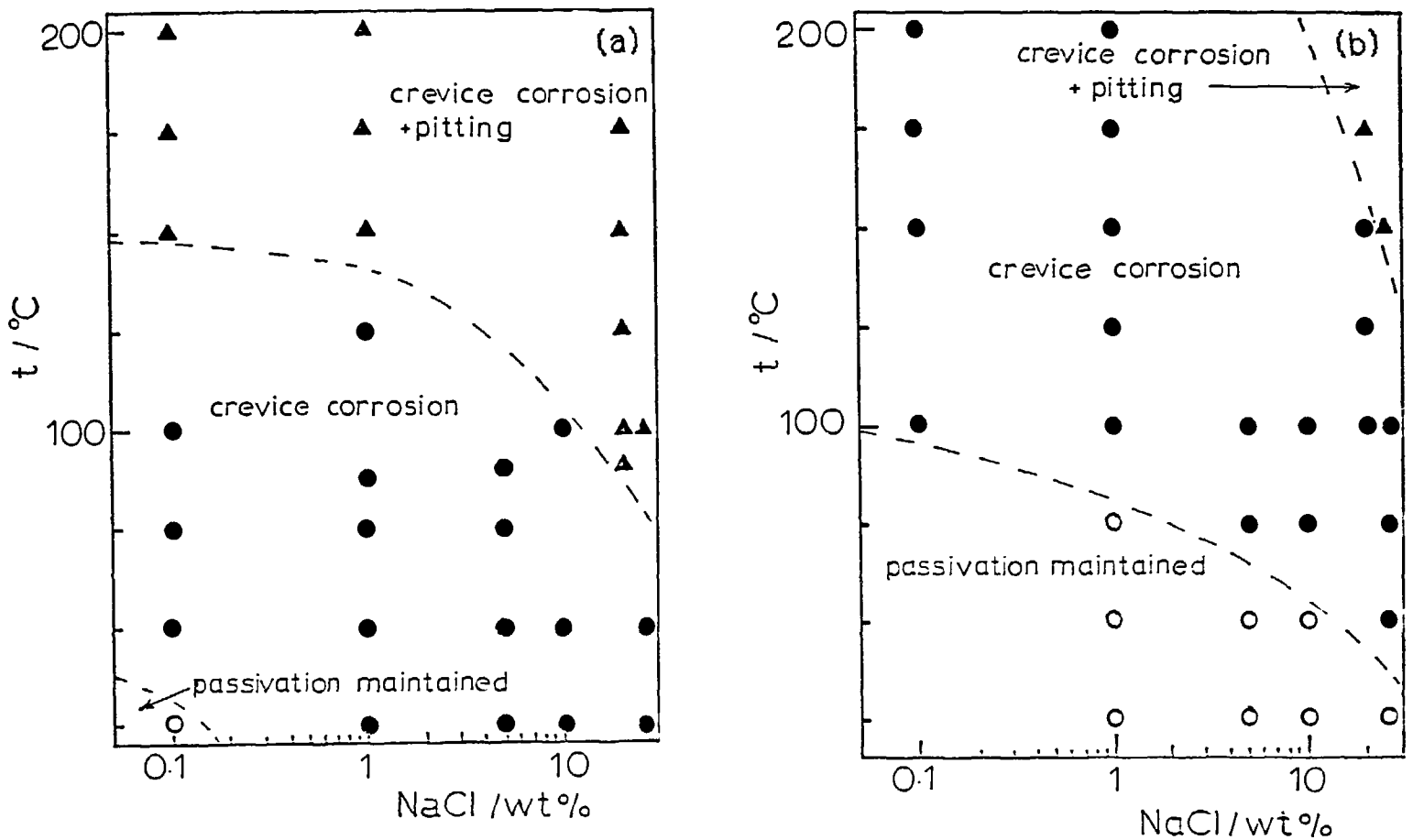

FIGURE 7: Susceptibility Diagrams for Various Corrosion Processes Determined from Cyclic Polarization Experiments; (a) Alloy 625; (b) Alloy C-276

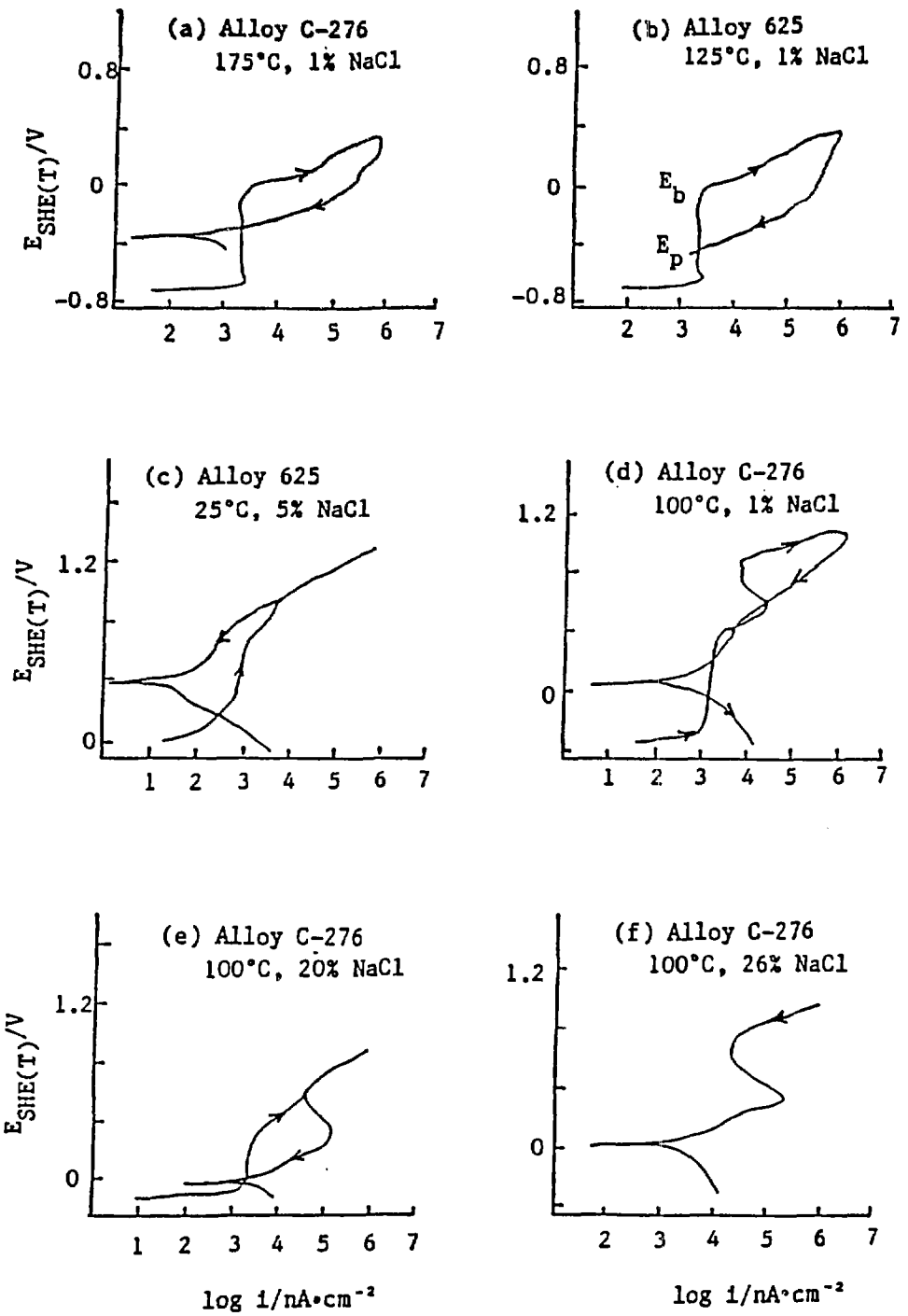

FIGURE 8: Cyclic Polarization Curves for Alloys C-276 and 625 in Chloride Solutions at Various Temperatures

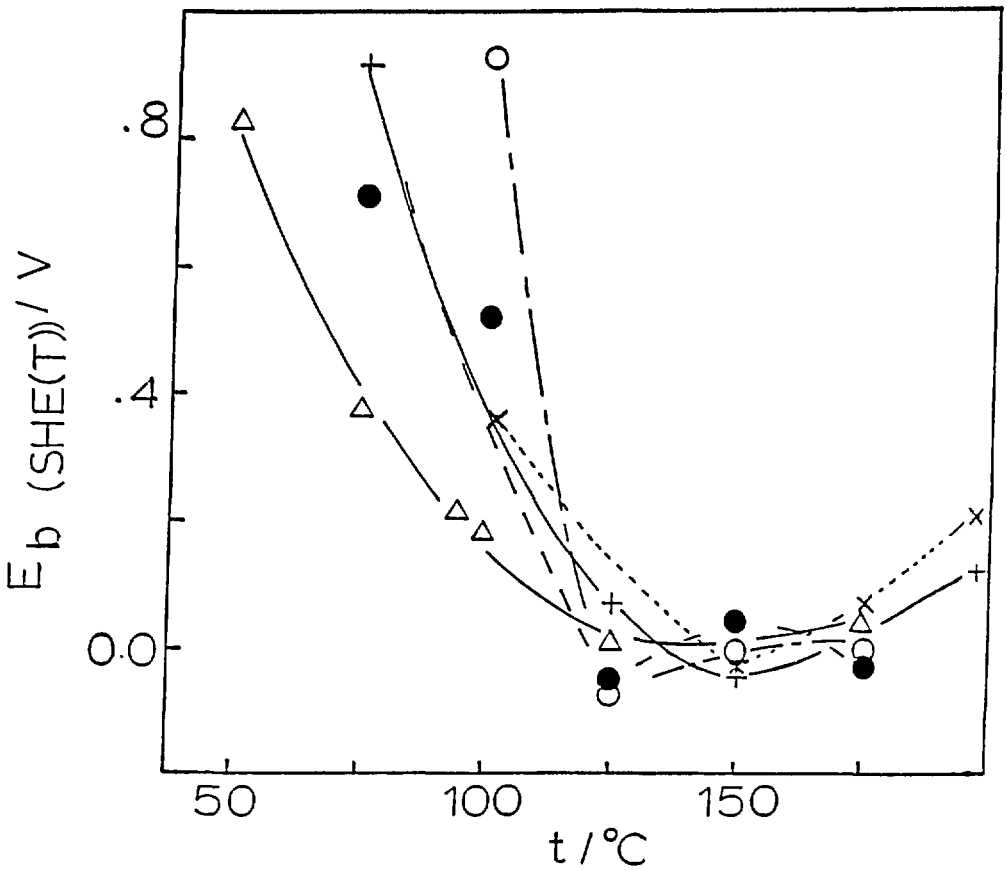

FIGURE 9: Passivation Breakdown Potentials from Cyclic Polarization Experiments as a Function of Temperature

+ = Alloy 625, 0.1 wt% NaCl
Δ = Alloy 625, 20.0 wt% NaCl
● = Alloy C-276 20.0 wt% NaCl
o = Alloy C-276, 1.0 wt% NaCl
X = Alloy C-276, 0.1 wt% NaCl

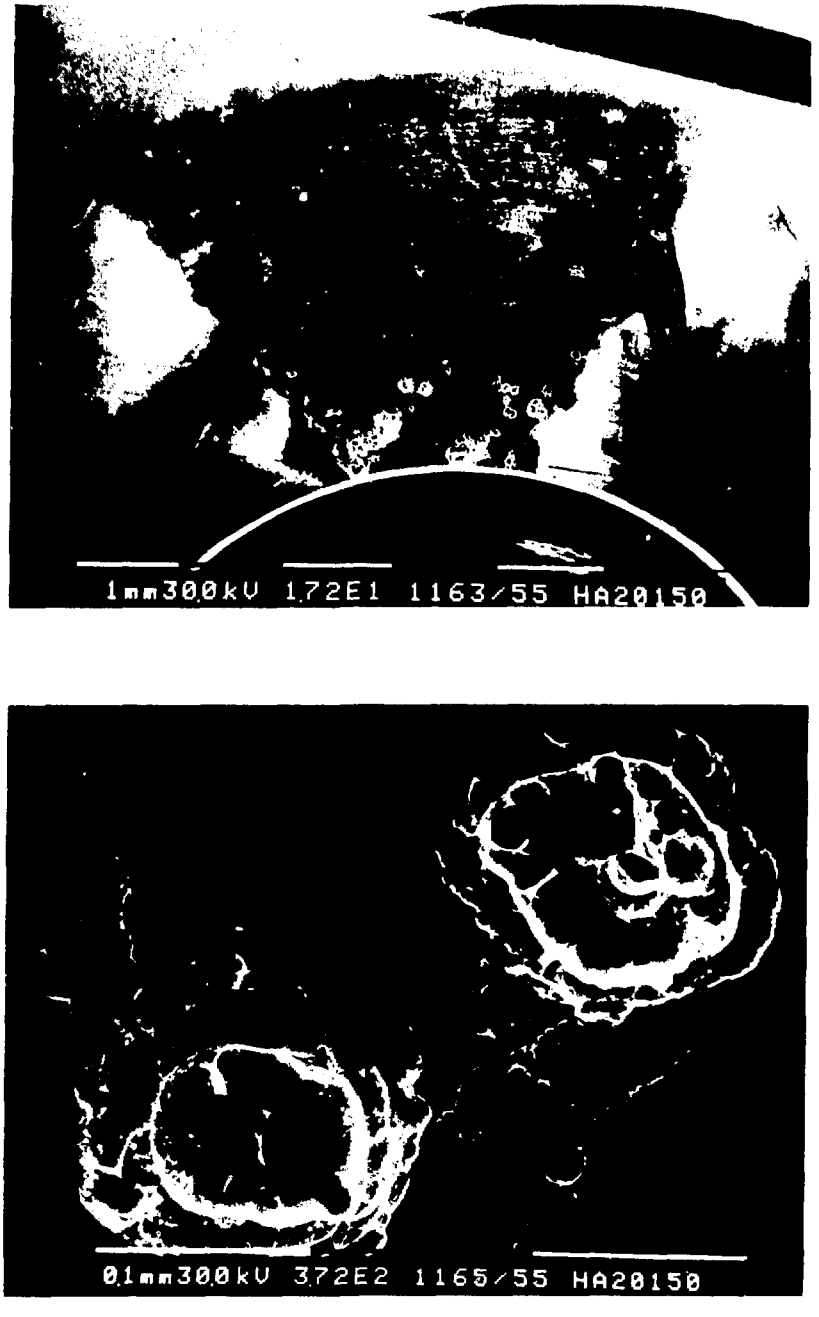

FIGURE 10: Photographs Showing the Crevice Corrosion of Alloy C-276 in Aerated 20 wt% NaCl at 150°C

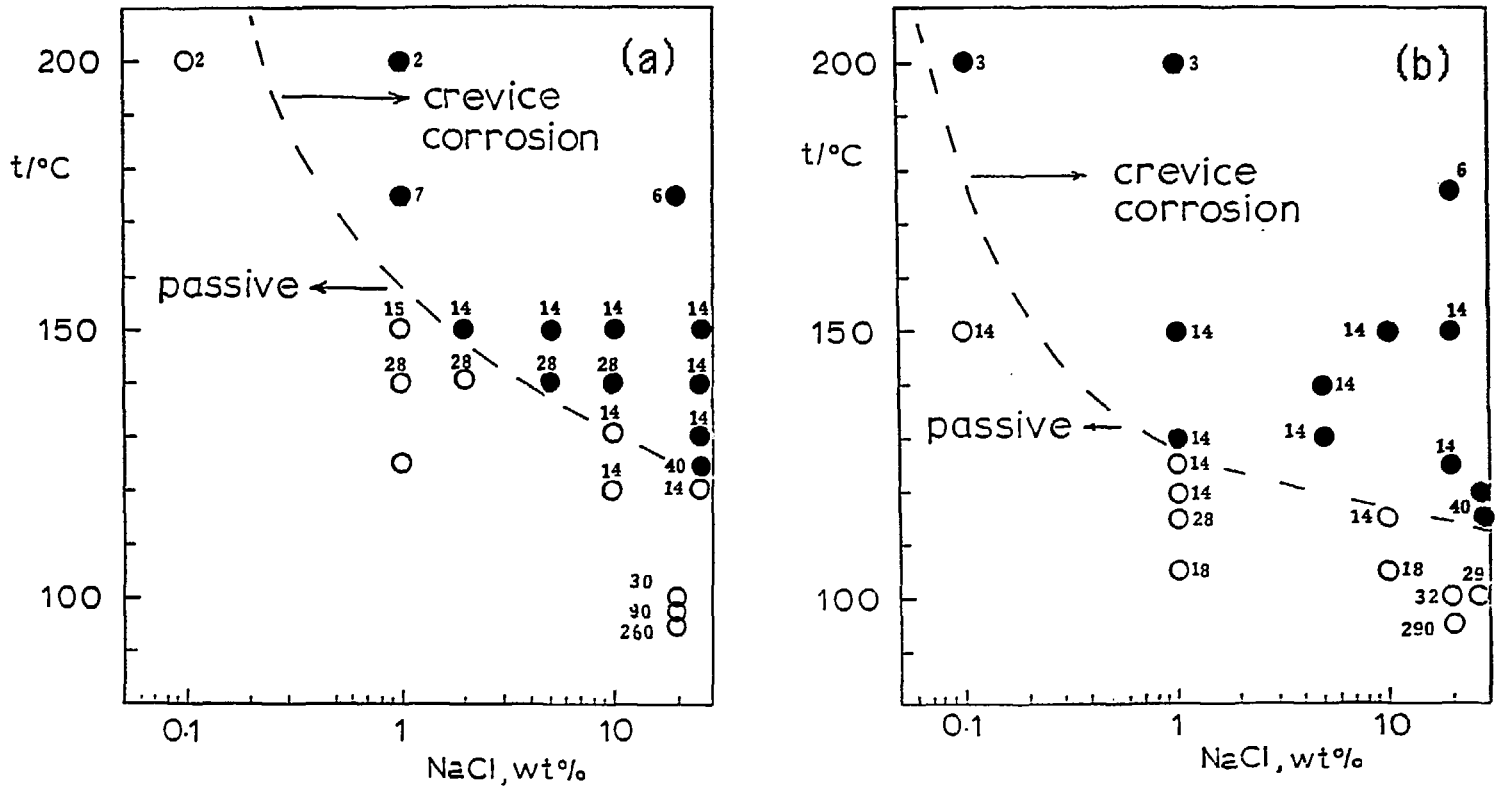

FIGURE 11: Crevice Corrosion Susceptibility Diagrams for (a) Alloy C-276 and (b) Alloy 625 in Aerated Solutions. The number beside each data point is the exposure time in days.

● = crevice corrosion with visible metal loss;
o = no visible corrosion;
--- = tentative crevice temperature envelope

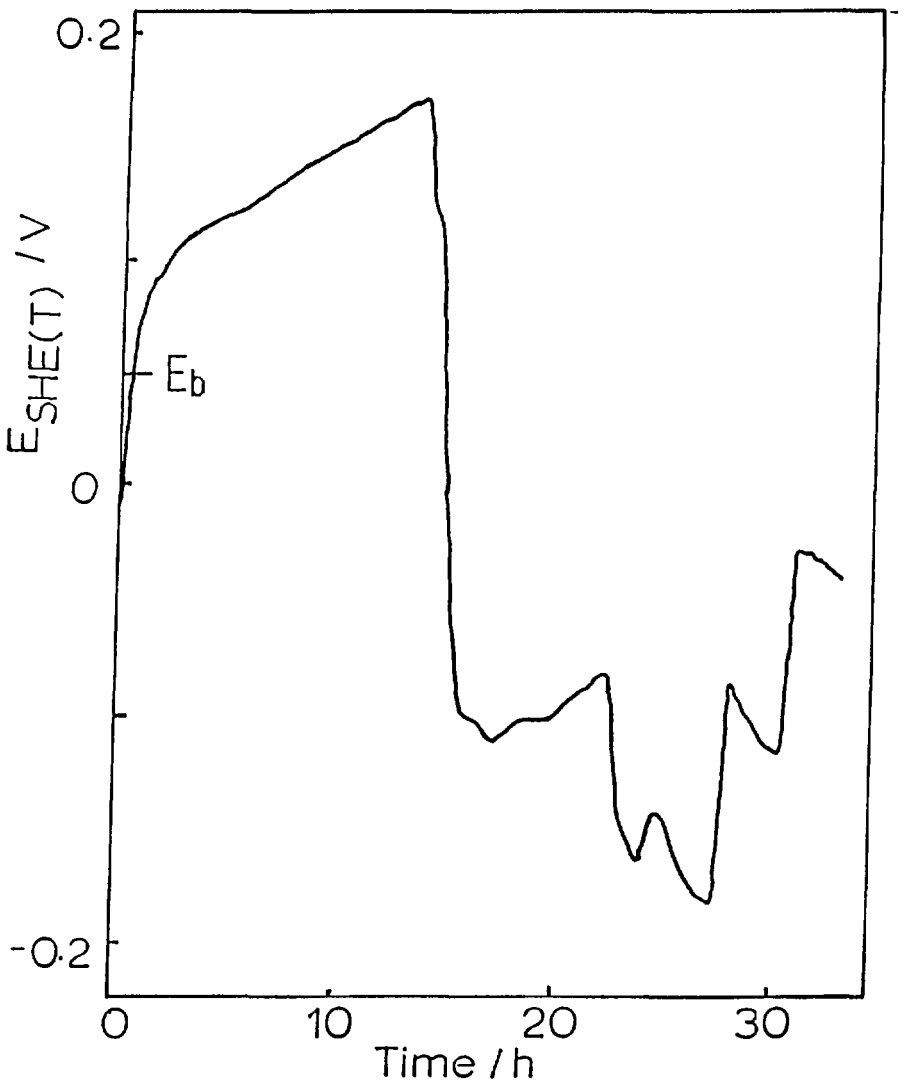

FIGURE 12: Corrosion Potential (E_{CORR}) Measured During Immersion Tests with Alloy 625 in 20 wt% NaCl at 125°C

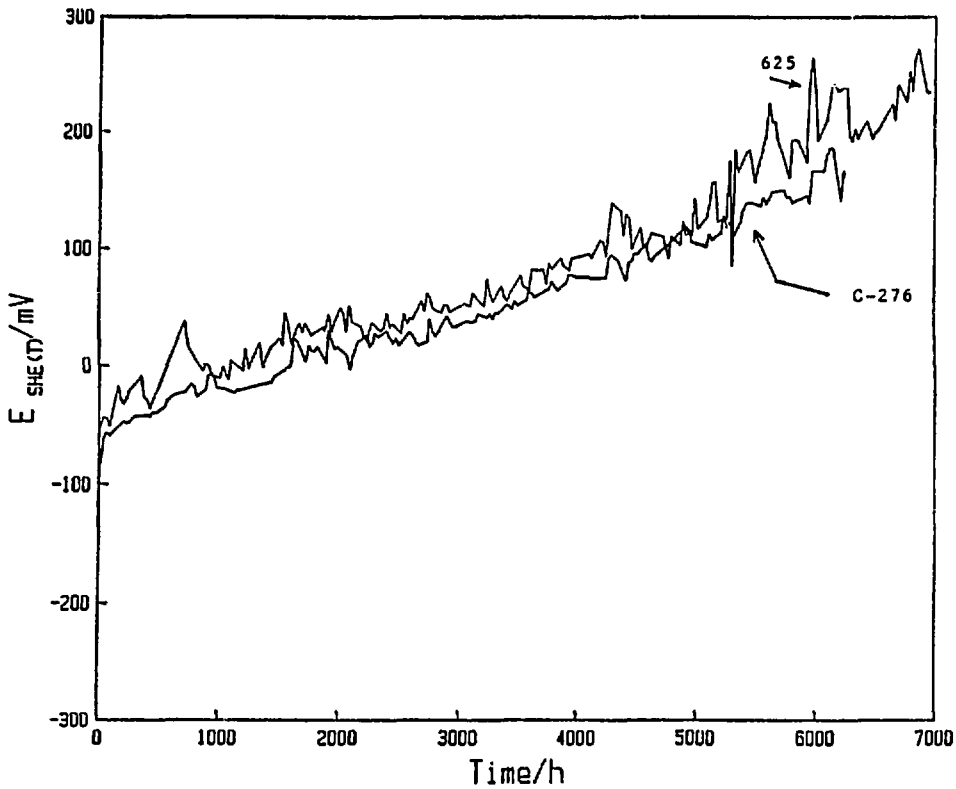

FIGURE 13: Corrosion Potential (E_{CORR}) Measured During Immersion Tests with Alloy C-276 and Alloy 625 in 20 wt% NaCl at 95°C

ISSN 0067-0367

To identify individual documents in the series, we have assigned an AECL- number to each.

Please refer to the AECL- number when requesting additional copies of this document

from

Scientific Document Distribution Office
AECL Research
Chalk River, Ontario, Canada
K0J 1J0

Price: A

ISSN 0067-0367

Pour identifier les rapports individuels faisant partie de cette série, nous avons affecté un numéro AECL- à chacun d'eux.

Veuillez indiquer le numéro AECL- lorsque vous demandez d'autres exemplaires de ce rapport

au

Service de Distribution des Documents Scientifiques
EACL Recherche
Chalk River, Ontario, Canada
K0J 1J0

Prix: A